Volume 8, Number 4 (August 2015) p. 447-466 • ISSN 1983-4195
http://dx.doi.org/10.1590/S1983-41952015000400002

REVISTA IBRACON DE ESTRUTURAS E MATERIAIS
IBRACON STRUCTURES AND MATERIALS JOURNAL

Construction of the interaction curve of concrete–encased composite columns based on the deformation domains of reinforced concrete sections

Construção da curva de interação para pilares mistos de aço e concreto totalmente revestidos com base nos domínios de deformação de seções de concreto armado

P. A. S. ROCHA [a]
paulorocha@em.ufop.br

K. I. DA SILVA [a]
katia@em.ufop.br

Abstract

This paper proposes a methodology for obtaining the interaction curve for composite steel–concrete sections subject to combined compression and bending based on the deformation domains of reinforced concrete structures defined by ABNT NBR 6118 [1]. For this, were developed expressions for the axial force, the moment and the strains of concrete, longitudinal reinforcement and the elements comprising the metal profile in each deformation domain. Based on these expressions a computer program called MDCOMP (2014) was created. In this study the same limit values of longitudinal reinforcement strain defined by ABNT NBR 6118 [1] were used for the steel profile strains. To verify the numerical implementations performed, the interaction curves and the plastic resistance of the section obtained by MDCOMP program were compared with those determined from the recommendations of Eurocode 4 [2], of ABNT NBR 8800 [3] or literature responses.

Keywords: composite steel–concrete columns, deformation domains, interaction curve, reinforced concrete.

Resumo

Neste trabalho se propõe uma metodologia para a obtenção da curva de interação para seções mistas de aço e concreto, sujeitas à flexão composta normal, com base nos domínios de deformação de estruturas de concreto armado definidos pela ABNT NBR 6118 [1]. Para isso, foram desenvolvidas expressões para o esforço normal, o momento fletor e para as deformações do concreto, das armaduras e dos elementos que compõem o perfil metálico em cada domínio de deformação. Com base nessas expressões criou–se um programa computacional denominado MDCOMP (2014). Neste trabalho utilizaram–se como valores limites das deformações do perfil metálico nos trechos comprimidos e tracionados, os mesmos estabelecidos pela ABNT NBR 6118 [1] para as deformações das armaduras de aço. Para verificar as implementações numéricas realizadas, as curvas de interação e os esforços máximos de plastificação da seção obtidos com o programa MDCOMP (2014) foram comparados com os determinados a partir das recomendações do EUROCODE 4 [2], da ABNT NBR 8800 [3] ou com respostas da literatura.

Palavras-chave: pilares mistos de aço e concreto, domínios de deformação, curva de interação, concreto armado.

[a] *Universidade Federal de Ouro Preto, Departamento de Engenharia Civil, Escola de Minas, Campus Morro do Cruzeiro.*

Received: 18 Nov 2014 • Accepted: 13 Apr 2015 • Available Online: 7 Aug 2015

1. Introduction

A composite steel–concrete system is every system in which a rolled, folded or welded steel profile works with reinforced concrete. Among the various systems, we can mention composite columns, beams, slabs and connections.

Composite structures appeared in the United States in the late nineteenth century, more precisely in 1894, with the initial purpose of protecting metals against corrosion and fire. Researches by Faber [4] and Jones and Rizk [5] allowed assessing the contribution of concrete to the structural performance of composite structural systems subject to axial loads (composite columns).

Some of the advantages of composite systems are, for instance, a considerable reduction of the structural steel consumption, the possibility of not needing forms and propping, a reduction of the own weight and volume of the structure and an increase in the dimensional accuracy of the construction. Moreover, when composite structures are compared with concrete and steel structures, there is an increase of the section's stiffness and strength, the elimination or reduction of local buckling in metal profiles, the protection against the profile's corrosion, and finally, an increased fire resistance especially in completely concrete encased columns.

Figure 1 shows two usual cross–sections of composite columns, one of which is partially encased with concrete and the other fully encased with concrete.

The mixing of concrete and steel in composite columns subject to simple compression or to the simultaneous action of axial compressive force and bending moments is also a way to leverage the advantages of both materials in order to find the best structural solution.

The first studies on composite steel–concrete columns date from the 60s. Jones and Rizk [5] studied the behavior of fully concrete encased columns taking into account variables such as column length, dimensions of the cross–section and volume of the piece reinforcement and, based on this study, they concluded that the concrete encased steel profile greatly contributed to increasing its load capacity, compared with a steel column.

In [6] the results of tests made with 22 composite columns fully encased with concrete, subject to bending around the lower inertia axis, with load applied by considering different eccentricities. The two failure modes observed after a certain applied load level were the concrete crushing on one side close to the top of the steel profile, and the concrete crushing on one side and the yielding of steel under compression, together with cracks in concrete on the opposite side.

Naka *et al.* [7] show the results of the experimental analysis of four composite columns with supported ends and subject to bending in relation to the greatest inertia axis. The results indicated that the failure mode of the columns was divided into two categories: concrete crushing and local buckling of the metal profile flange in the compressed side; concrete crushing, buckling of the steel reinforcements under compression and yielding of the reinforcements on the tensioned side.

Yamada *et al.* [8] analyzed composite columns subject to the combination of axial forces and transverse loads applied to the extremities of the column, considering bending of the structural system in relation to the greatest inertia axis. In most models studied, there was a reduction in the maximum load capacity of the column when the concrete started cracking and the reinforcement bars started yielding in the tensioned region.

Ricles and Paboojian [9] show the experimental results of eight composite columns fully encased with concrete, with cross–section dimensions equal to 406mmx406mm and shear connectors. Columns were subject to bending in relation to the greatest inertia axis and tested under monotonic axial load and cyclic lateral load. It was verified that the maximum load caused the yielding of the metal profile flange and of the reinforcing bars, and that shear connectors were not effective in improving the flexural strength.

Mirza *et al.* [10] studied the behavior of sixteen 4m long columns, fully encased with concrete, subject to bending in relation to the greatest inertia axis, taking into account the second order effects in the analysis. The tests carried out showed that the concrete strain in the most compressed fiber ranged from 0.0025 to 0.004 before the models collapsed. The presence of shear connectors had little influence on the ultimate capacity of the composite column.

Figure 1 – Composite sections partially and fully encased with concrete

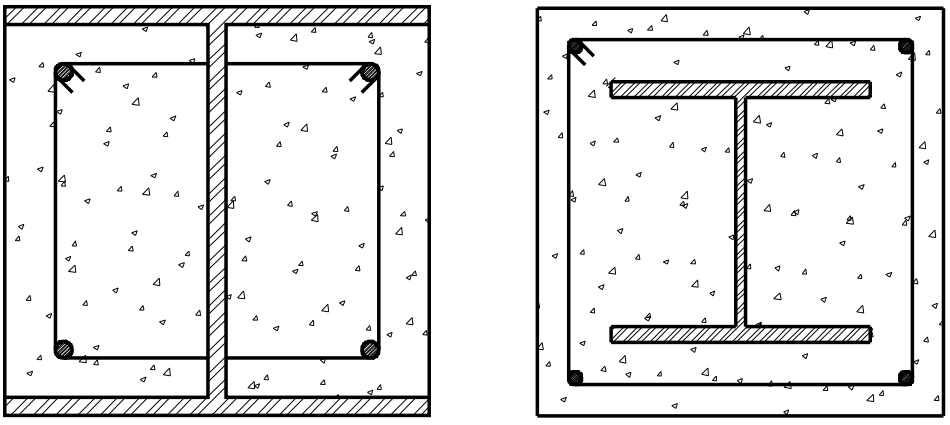

Yokoo *et al.* [11] performed experimental analysis on nineteen short composite columns fully encased with concrete with $f_{ck} = 30\,MPa$. In this experimental program, large cracks were identified on the lower side of the models and the failure occurred due to concrete crushing. The conclusion was that short columns show a failure mechanism characterized by the yielding of steel and concrete crushing and thus are not influenced by second order effects.

Slender columns, in turn, are subject to geometric imperfections capable of amplifying acting forces, resulting in buckling and characterizing the so-called stability criterion. They behave inelastically and fail due to the partial inelasticity of steel, concrete crushing in the compressed region and cracking of concrete in the tensioned region.

Other important effects in those structures such as ductility and energy dissipation capacity of composite columns fully encased with concrete have been investigated and are being explored in Japan and North America. Among some important works, we can mention the researches carried out by Wakabayashi *et al.* [12, 13].

Liew *et al.* [14] demonstrated, from studies on composite columns partially and fully encased with concrete, that the results of the design of composite columns defined by Eurocode 4 [2], British code BS 5400 [15] and AISC/LRFD [16] were not necessarily the same. Such differences have been attributed to different values of load and resistance factors and to the design considerations regarding creep concrete and load eccentricity.

Saw and Liew [17] presented the evaluation of the design of composite columns with I sections partially and fully encased with concrete and with tubular sections filled with concrete, based on criteria established by Part 1.1 of Eurocode 4 [2], by part 5 of British code BS 5400 [15] and by the American code AISC/LRFD [16]. In this research, design parameters were studied and comparisons were made between the nominal strength predicted by the three codes and the predicted strengths with the experimental tests results. In some cases, the results obtained from normative codes varied considerably due to different project considerations regarding each code. However, design procedures in general showed more conservative responses when compared with the results of experimental tests. In turn, EUROCODE 4 [2] presents important favorable factors in terms of its scope and broad range of application.

For columns subject to pure compression, concrete strain limit is of 0.2%. Thus, in order to prevent the premature collapse of the concrete in the element, the steel strain of the profile and reinforcements shall also be limited to this value [18].

Weng and Yen [19] investigated the differences between the approaches of code ACI 318 [20] and AISC/LRFD [16] for the design of composite steel–concrete columns fully encased with concrete and evaluated how their results were close to the responses of a real column. This was confirmed by a series of statistical comparisons. Studies were conducted in order to compare estimated relevant issues using the codes ACI 318 [20] and AISC/LRFD [16]. These approaches were compared with results of composite columns fully encased with concrete obtained in previous researches. Among such researches, we may mentioned the physical tests conducted by Stevens [6], Naka et al. [7], Yamada et al. [8], Ricles and Paboojian [9], Mirza et al. [10], Yokoo et al. [11] and Wakabayashi et al. [12].

Figure 2 – Deformation domains for reinforced concrete sections

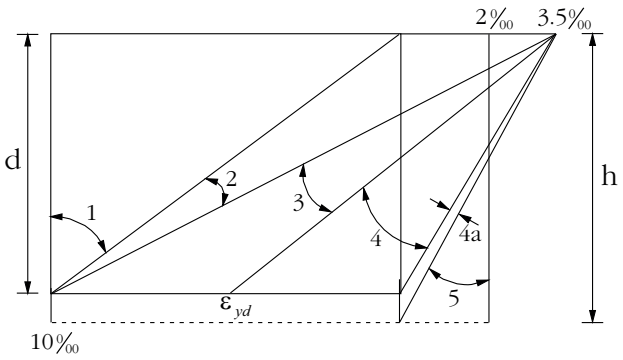

Among the numerical modeling of composite steel–concrete columns, Fong [21] points out that many codes tend to recommend the use of a second order analysis and design method to efficiently obtain more accurate results. Some recent studies were developed to obtain numerical formulations for advanced analysis of composite steel–concrete structures, based on the refined plastic hinge method.

An effective numerical procedure for the construction of the interaction curve of composite steel–concrete columns is the fiber method consisting in the subdivision of the cross–section area in smaller single material regions, distributed along the length of the column [22].

In this paper, we propose a calculation procedure based on the deformation domains of reinforced concrete sections, as shown in Figure 2, to obtain the interaction curve of composite columns fully encased with concrete in a computational manner. This approach was adopted due to the similarities found between the interaction curves of reinforced concrete sections and composite steel–concrete sections. The computational package developed is called MDCOMP (2014) and was implemented in FORTRAN language. Results obtained using MDCOMP (2014) are compared with the responses defined by Part 1.1 of Eurocode 4 [2], which is one of the most important codes used to design this type of structural element, and also with the answers presented in the works of Saw and Liew [17], Weng and Yen [19] and Naka et al. [7].

2. Interaction curve of composite column cross section

The interaction curve is the geometric locus of M–N pairs that define the limits of strength of the cross–section of a structural member under combined compression and bending.

Figure 3 shows the curve adopted by Part 1.1 of Eurocode 4 [2], as well as the simplified polygonal diagram adopted by NBR 8800 [3], which is represented by the dotted curve in Figure 3. In this case, we shall consider that there is a total plastic stress distribution between points A, which corresponds to the maximum axial force, and D, which is the maximum bending moment.

At point A, the interaction curve has only the contribution of the

Figure 3 – Interaction curve according to EUROCODE 4 (2)

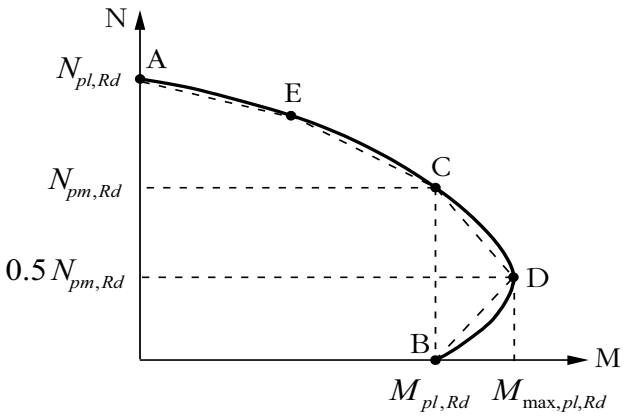

axial force on the piece, thus concrete, metal profile and steel reinforcements are subject to compressive normal force, with

$$N_A = N_{pl,Rd} \quad \text{and} \quad M_A = 0 \tag{1a}$$

At point B, column is subject only to pure bending, where

$$N_B = 0 \quad \text{and} \quad M_B = M_{pl,Rd} \tag{1b}$$

At point C, we find the combination of axial load and bending, i.e.,

$$N_C = N_{pm,Rd} = \frac{0.85\,A_c\,f_{ck}}{\gamma_c} \quad \text{e} \quad M_C = M_{pl,Rd} \tag{1c}$$

and at point D, we see

$$N_D = 0.5\,N_{pm,Rd} = 0.5\,\frac{(0.85A_c\,f_{ck})}{\gamma_c} \quad \text{and} \quad M_D = M_{\max,pl,Rd} \tag{1d}$$

$$M_{Pl} = \frac{Z_{Pa}\,f_y}{\gamma_a} + \frac{Z_{Ps}\,f_s}{\gamma_s} + \frac{1}{2}\,\frac{Z_{Pc}(0.85\,f_{ck})}{\gamma_c} \tag{1e}$$

Point E is located on the average point of the curve between points A and C.

In the above equations, $N_{pl,Rd}$ is the design value of the plastic resistance of the composite section to compressive normal force, $N_{pm,Rd}$ is the design value of the resistance of the concrete to compressive normal force, $M_{pl,Rd}$ is the design value of the plastic resistance moment of the composite section and Z_{Pa}, Z_{Ps}, Z_{Pc} are, respectively, the plastic resistance modulus of steel profile, reinforcement bars and concrete.

3. Definition of balance and deformation equations

Figure 4 schematically shows the strain diagram of the composite section fully encased with concrete, as well as the resulting forces acting on the section.

Figure 4 – Composite section and strain diagram with scheme of resultant forces

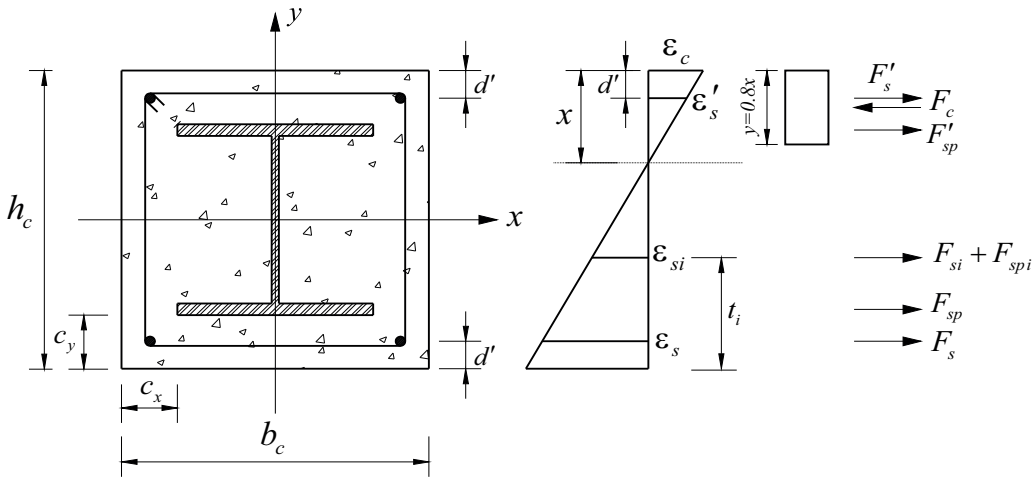

In this figure, F'_s, F'_{sp}, F_{si}, F_{spi}, F_{sp} and F_s are, respectively, the resulting forces on the upper reinforcements of the composite section, on the top flange of the metal profile, on the generic reinforcements located between the profile flanges, on the web of the metal profile, on the bottom flange of the metal profile and on the bottom reinforcements of the composite section.
Considering the equilibrium of normal force and bending moment in the section, we find:

$$N_{Rd} = -F_c + \sum_{i=1}^{n} F_i \quad (2)$$

$$M_{Rd} = N_d \frac{h}{2} + F_c (h - 0.4\,x) - \sum_{i=1}^{n} F_i t_i \quad (3)$$

The sums of the equations above correspond to the contributions of forces and bending moments of concrete, reinforcements and metal profile.
The position of the neutral axis of the composite section (x) is defined based on the relation

$$x = \frac{\varepsilon_c}{\varepsilon_c + \varepsilon_s} \quad (4)$$

where ε_c is the concrete strain, ε_s is the lower reinforcement's steel strain and d' is the distance from the centroid of steel reinforcements and the edge of the composite steel–concrete section, which results from:

$$d' = c + \phi_t + 0.5\phi_l \quad (5)$$

In Eq. 5, c is the thickness of concrete cover, ϕ_t is the diameter of the transverse reinforcement (stirrups) and ϕ_l is the diameter of the longitudinal reinforcement.
Equations that relate the strain of steel reinforcements and of the elements making up the metal profile with concrete strain are:

$$\varepsilon'_s = \frac{\varepsilon_c (x - d')}{x} \quad (6a)$$

$$\varepsilon_s = -\frac{\varepsilon_c (d - x)}{x} \quad (6b)$$

$$\varepsilon'_{sp} = \frac{\varepsilon_c (x - c_y - 0.5\,t_f)}{x} \quad (6c)$$

$$\varepsilon_{sp} = -\frac{\varepsilon_c (h_c - x - c_y - 0.5\,t_f)}{x} \quad (6d)$$

$$\varepsilon_{spi} = -\frac{\varepsilon_c (d - x + d' - 0.5\,h_c)}{x} \quad (6e)$$

In the above equations, ε'_s and ε_s are, respectively, the strains of upper and lower steel reinforcements, ε'_{sp} and ε_{sp} are the strains of the upper and lower flange of the metal profile, respectively, ε_{spi} is the strain of the metal profile web, d is the distance between the steel reinforcement in tension to the extreme fiber of the composite section on the compressed side (effective height of the composite section), c_y is the thickness of concrete cover and h_c is the depth of the concrete encasement to a steel section (see Fig. 4).
In this study, the strain of steel reinforcements and metal profile were limited to 1% in traction and 0.35% in compression, as determined by ABNT NBR 6118 [1], since concrete does not show strains beyond these limits.
As in domain 5, the neutral axis is outside the reinforced concrete section, i.e., $h_c < x < +\infty$, ensuring the equilibrium of forces and moments in the section, not taking into account the strength portion corresponding to reinforcements, and setting the moment equation equal to zero, the limit amount of the neutral axis position in this domain is reached and equal to $x = 1.25h$.
The limit value x for the composite steel–concrete section was obtained in a manner similar to that described above for the reinforced concrete section, but considering the portion of strength related to concrete and metal profile. Thus, the equilibrium of forces and moment on section provides:

$$N_{Rd} = -F_c + A_a f_{yd} \quad (7)$$

and

$$M_{Rd} = N_{Rd} \frac{h}{2} + F_c (h - 0.4\,x) \quad (8)$$

Figure 5 – Interaction curve of the cross-section of a reinforced concrete column

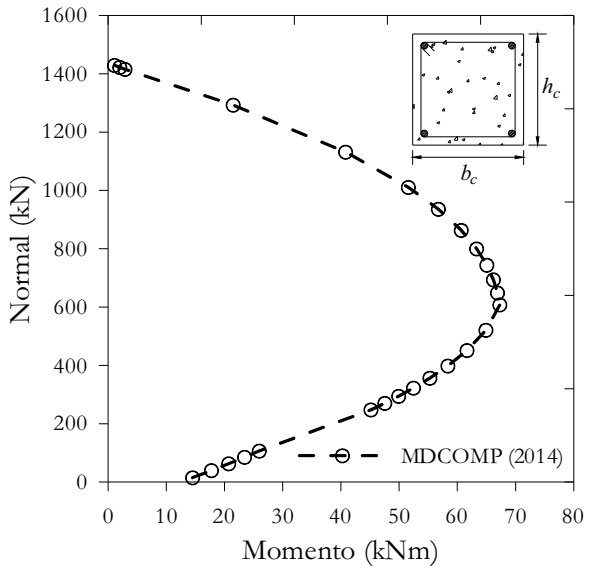

By substituting (7) by (8) and doing $M_{Rd} = 0$, taking into account that Fc = 0.85 fcd b x, we reach the following second degree equation:

$$0 = 0.85 f_{cd}\, b\, 0.8 x\, (0.5 h - 0.4 x) + A_a\, f_y\, 0.5 h \qquad (9)$$

The largest root of equation (9), x = 2.305h, corresponds to a null value for the bending moment and to the maximum value for the axial force in the section and is, therefore, the limit value for the position of the neutral axis of the composite steel–concrete section.

4. Examples

This section presents the interaction curves of cross–sections of a reinforced concrete column and various cross–sections of composite steel–concrete columns obtained numerically from the computer program MDCOMP (2014). Comparisons are made, where possible, with the curves obtained according to current codes and/or with the answers provided by other researchers.

Table 1 – Sizes of concrete cross-section

Composite section	h_c (mm)	b_c (mm)	c_y (cm)	$\rho_s = \frac{A_a}{A_c}$ %
SM1	333	334	4.0	8.33
SM2	403	454	7.5	5.10
SM3	553	654	15.0	2.56

4.1 Interaction curve of the cross–section of a reinforced concrete column

In this example, we analyze the cross–section of a reinforced concrete column with section $33.3\,cm \times 33.4\,cm$. The concrete has $f_{ck} = 20MPa$ and longitudinal reinforcement consists of four CA50 steel bars with a $\phi_l = 10\,mm$ diameter, as to know $d' = 3.5\,cm$. Figure 5 shows the interaction curve moment x normal for the section obtained from the variation of the concrete and steel strains within the six deformation domains (see Figure 2). The portion of the curve corresponding to combined tension and moment, which includes domain 1 and a portion of domain 2, was deleted, i.e., only portions referring to the section behavior under compression and bending are presented.

4.2 Interaction curve of the cross–section of a composite steel–concrete column

In this example, we find the analysis of the cross–section of a composite steel–concrete column formed by a Gerdau rolled metal profile $W250 \times 73\,kg/m$ and considering three different values for the depth and width of the concrete encasement to the steel section, i.e., h_c and b_c, as shown in Table 1.
In Table 1, ρ_s is the ratio of the area of the steel profile cross–section (A_a) and the area of the concrete cross–section (A_c).
The concrete used has $f_{ck} = 20MPa$, four CA50 steel bars with a $\phi_l = 10\,mm$ diameter for the longitudinal reinforcement and $d' = 3.5\,cm$.

Figure 6 – Interaction curve of cross-sections of composite steel-concrete column

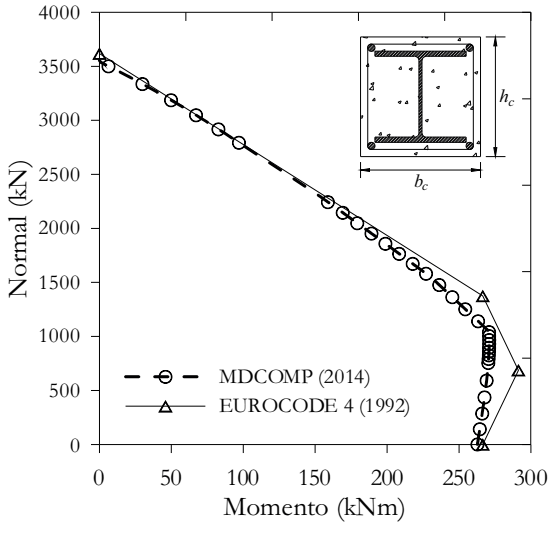

Figure 6b – Interaction curve of cross-sections of composite steel-concrete column

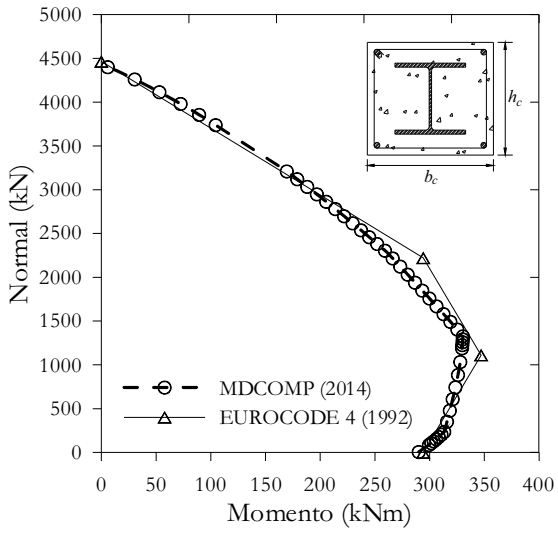

B Section SM2

Figure 6c – Interaction curve of cross-sections of composite steel-concrete column

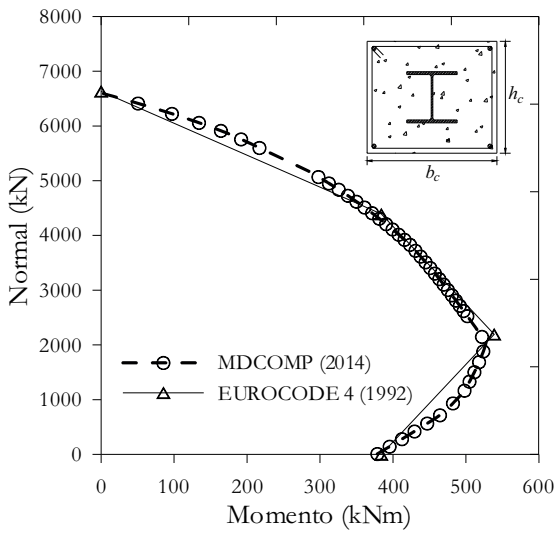

C Section SM3

In the graphs shown in Figure 6, we see the interaction curves moment x normal obtained with the MDCOM computational package (2014) for the three composite steel–concrete sections, being compared to the curves obtained based on the EUROCODE 4 [2] considerations.

Tables 2 and 3 show, respectively, the numerical results of design value of the resistance to moment and normal force to the composite steel–concrete section and comparisons with responses obtained based on the recommendations of Eurocode 4 [2].

4.3 Comparison with results found in books

In this section, we make a comparison between the results of the MDCOMP computer program (2014) and the responses obtained by other researchers or from current codes.

The first interaction curves shown refer to the cross–section of a composite steel–concrete column previously analyzed by Saw and Liew [17] in accordance with the recommendations of Eurocode 4 [2]. The section is formed by a $UC\,254\times254\times107\,kg/m$ steel profile with $f_y = 355MPa$, four steel bars with $f_{yk} = 460MPa$ and longitudinal reinforcement with $\phi_l = 12.5\,mm$, concrete with $f_{ck} = 20MPa$ and $b_c = h_c = 400\,mm$ dimensions.

The interaction curves obtained in this analysis are presented in Figure 7.

Table 4 presents the comparisons between the resistant capabilities obtained with the MDCOMP program (2014) and the ones obtained by Saw and Liew [17].

The second comparison was made with an interaction curve obtained from the recommendations of the American code ACI 318 [20]. For this analysis, we used a section with $b_c = h_c = 240mm$ ($f_{ck} = 25.6\,MPa$), which fully covers a metal profile $H96\times100\times5.1\times8.6\,mm$ ($f_y = 311.2\,MPa$ and four steel bars

Table 2 – Maximum design value of the plastic resistance moment ($M_{max,pl,Rd}$) and design value of the plastic resistance moment ($M_{pl,Rd}$)

Composite section	$M_{max,pl,Rd}$ (kNm)			$M_{pl,Rd}$ (kNm)		
	EC4	MDCOMP	$\frac{M_{MDCOMP}}{M_{EC4}}$	EC4	MDCOMP	$\frac{M_{MDCOMP}}{M_{EC4}}$
SM1	291.28	270.44	0.93	291.28	270.44	0.99
SM2	346.98	330.31	0.95	346.98	330.31	0.99
SM3	538.63	527.49	0.98	538.63	527.49	0.99

Table 3 – Design value of the plastic resistance to compressive normal force ($N_{pl,Rd}$)

Composite section	$N_{pl,Rd}$ (kN)		
	EC4	MDCOMP	$\frac{N_{MDCOMP}}{N_{EC4}}$
SM1	3618.22	3553.66	0.98
SM2	4465.09	4430.69	0.99
SM3	6635.02	6602.54	0.99

with $f_{yk} = 634\,MPa$ and $\phi_l = 10\,mm$ for longitudinal reinforcements. We found $\rho_s = 3.7\%$ and $\rho_r = 0.5\%$, where ρ_r is the steel rate of the longitudinal reinforcement ($\rho_r = A_s / A_c$). Results are shown in Figure 8.

Table 5 shows comparisons between the resistant capabilities obtained with the MDCOMP program (2014) and the ones defined by the American code ACI 318 [20].

In the last analysis, another comparison of MDCOMP program (2014) results was made with those obtained from the recommendations of the American code ACI 318 [20] and with the experimental results presented by Naka *et al.* [7].

The analyzed cross–section is formed by a steel profile $H\,180 \times 120 \times 4.5 \times 12\,mm$ ($f_y = 344.8\,MPa$) encased with concrete with $f_{ck} = 25.5\,MPa$, and $b_c = 240\,mm$ and $h_c = 300\,mm$ dimensions. Four steel bars $f_{yk} = 461.3\,MPa$ and $\phi_l = 10\,mm$ were used for longitudinal reinforcement. We found $\rho_s = 4.6\%$ and $\rho_r = 3.2\%$. Graphs in Figure 9 show the interaction curves obtained in this analysis.

Table 4 – Parameterized maximum design value of the plastic resistance moment ($M_{max,pl,Rd}$), design value of the plastic resistance moment ($M_{pl,Rd}$) and design value of the plastic resistance to compressive normal force ($N_{pl,Rd}$)

Force	EC4	MDCOMP	$\frac{MDCOMP}{EC4}$
$M_{max,pl,Rd}/M_u$	0.97	0.92	0.95
$M_{pl,Rd}/M_u$	0.90	0.89	0.99
$N_{pl,Rd}/N_u$	0.92	0.96	1.04

5. Conclusions

In this paper, we presented a methodology that allows the construction of the interaction curve for composite steel–concrete sections subject to combined compression and bending, based on the deformation domains of reinforced concrete structures defined by ABNT NBR 6118 [1]. To this end, relationships were described for the strains of reinforcements and elements comprising the metal profile, according to the strains of concrete, as well as equations for the normal force and bending moment in each deformation domain. From these expressions, the M–N pairs were determined in the ultimate limit state, needed to build the interaction curve.

Tables 2 to 5 show that the design value of the plastic resistance to compressive normal force ($N_{pl,Rd}$), the design value of the plastic resistance moment ($M_{pl,Rd}$) and the maximum design value of the plastic resistance moment ($M_{max,pl,Rd}$) of the composite section

Figure 7 – Interaction Curves – MDCOMP (2014) x Saw and Liew (2000)

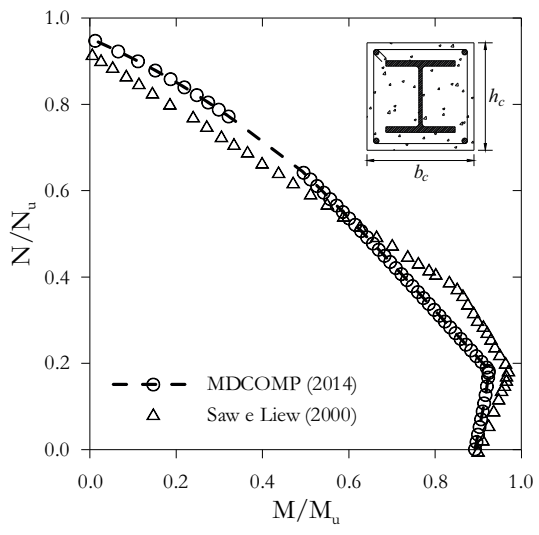

Figure 8 – Interaction Curves – MDCOMP (2014) x ACI 318 (1999)

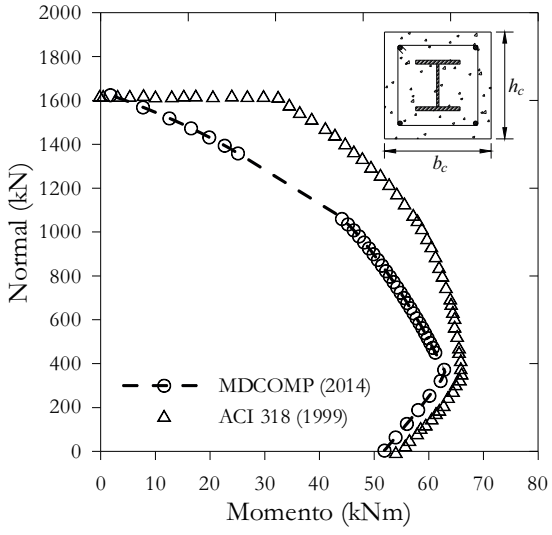

Table 5 – Maximum design value of the plastic resistance moment ($M_{max,pl,Rd}$), design value of the plastic resistance moment ($M_{pl,Rd}$) and design value of the plastic resistance to compressive normal force ($N_{pl,Rd}$)

Force	ACI 318	MDCOMP	MDCOMP / ACI318
$M_{max,pl,Rd}$ (kNm)	66.00	62.91	0.95
$M_{pl,Rd}$ (kNm)	53.95	51.88	0.96
$N_{pl,Rd}$ (kN)	1622.19	1644.11	1.01

obtained from MDCOMP computer program (2014), which is based on relationships defined by NBR 6118 [1], are very close to those set by both the EUROCODE 4 [2] and ACI 318 [20]. From the graph in Figure 9, we can find that in the comparison between the experimental results of Naka *et al.* [7], the approach of ACI 318 [20] provides more precisely than the procedure based on deformation domains recommended by NBR 6118 [1], although the results corresponding to maximum resistances ($N_{pl,Rd}$ and $M_{pl,Rd}$) are very similar in the two processes.

With regard to the variation rate of the steel in the metal profile in the composite section (ρ_s), we may verify that the smaller the value, the more the curve approaches the theoretical graphic for composite steel–concrete columns defined by EUROCODE 4 [2] (see Figure 6 and Tables 2 and 3). This is evidenced by comparing curve in Figure 6c with curve in Figure 3.

Finally, it is clear from the examples analyzed that the numerical results obtained via MDCOMP (2014) showed a good correlation with the interaction curves defined by Eurocode 4 [2], but there were some discrepancies with the answers defined by ACI 318 [20] (see Figures 8 and 9). This is due to the different values of partial safety factors for strength and loads, as well as to design considerations regarding creep concrete and load eccentricity adopted by each code.

Figure 9 – Comparison of interaction curves

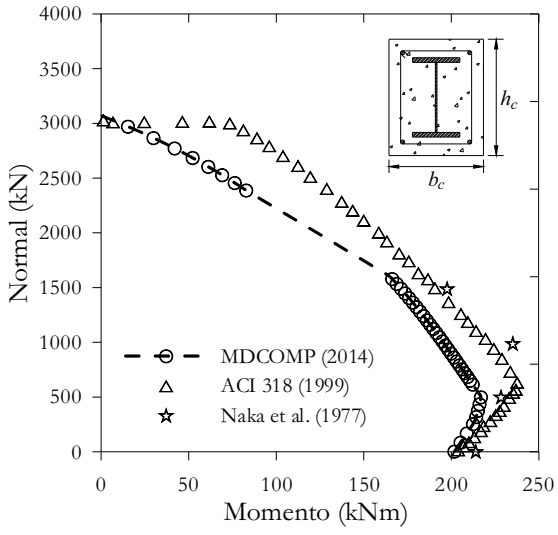

6. References

[1] ASSOCIAÇÃO BRASILEIRA DE NORMAS TÉCNICAS (2003), NBR 6118:2003. Projeto de estruturas de concreto armado. Rio de Janeiro, RJ.

[2] EUROPEAN COMMITTEE FOR STANDARDIZATION (1992), EUROCODE 4, Design of composite steel and concrete structures – Part 1.1: General rules and rules for buildings, CEN, Bruxelas, Belgium.

[3] ASSOCIAÇÃO BRASILEIRA DE NORMAS TÉCNICAS (2008), NBR 8800:2008. Projeto e execução de estruturas de aço e de estruturas mistas aço–concreto de edifícios: Projeto de revisão. Rio de Janeiro.

[4] Faber, O. (1956), Savings to be affected by the more rational design of encased stanchions as a result of recent full size tests, The Structural Engineer, vol. 34, pp. 88–109.

[5] Jones, R. and Rizk, A.A. (1963), An investigation on the behaviour of encased steel columns under load, The Structural Engineer, Vol. 41, N° 1, pp. 21–33.

[6] Stevens, R.F. (1965), Encased stanchions, The Structural Engineer, 43(2), pp. 59–66.

[7] Naka, T., Morita, K. and Tachibana, M. (1977), Strength and hysteretic characteristics of steel–reinforced concrete columns (in Japanese), Transaction of AIJ; 250, pp. 47–58.

[8] Yamada, M., Kawamura, H., and Zhang, F. (1991), Research on the elasto–plastic deformation and fracture behaviors of wide flange steel encased reinforced concrete columns subjected to bending and shear (in Japanese), Journal of Structural Construction Engineering, AIJ Architectural Institute of Japan); 420, pp. 63–74.

[9] Ricles, J.M. and Paboojian, S.D. (1994), Seismic performance of steel–encased composite columns, Journal of Structural Engineering, ASCE; 120(8), pp. 2474–2494.

[10] Mirza, S.A., Hyttinen, V. and Hyttinen, E. (1996), Physical tests and analyses of composite steel–concrete beam–columns, Journal of Structural Engineering, ASCE; 122(11), pp. 1317–1326.

[11] Yokoo, Y., Wakabayashi, M. and Suenaga Y. (1967), Experimental studies on steel concrete members with H–shape steel (in Japanese). Transaction of AIJ; 136, pp. 1–7.

[12] Wakabayashi, M., Shibata, M., Matsui, C. and Minami, K. (1974), A study on the behaviour of steel–reinforced concrete columns and frames. In: IABSE Symposium, pp. 53–60.

[13] Wakabayashi, M. (1987), A historical study of research on composite construction in Japan. In: Composite construction in steel and concrete. Proc. of eng. foundation conf. Henniker, New Hampshire: ASCE, pp. 400–427.

[14] Liew, J.Y.R., Saw, H.S. and Yu, C.H. (1998), Composite column design in buildings – Assessment of current methods and interim guidance. Research Report n. CE 026/98, National University of Singapore, May.

[15] BS 5400 (1979), Steel, concrete and composite bridges,

Part 5, Code of practice for design of composite bridges. London: British Standards Institution.

[16] AISC/LRFD (1993), Load and Resistance Factor Design Specification for Structural Steel Buildings, 1st edn., American Institute of Steel Construction, AISC, Chicago, IL.

[17] Saw, H.S. and Liew, J.Y.R. (2000). Assesment of Current Methods for the Design of Composite Columns in Buildings. Journal of Constructional Steel Research, v. 53, p. 121–147.

[18] Queiroz, G., Pimenta, R.J. and Da Mata, L.A.C. (2001), Elementos das Estruturas Mistas Aço–Concreto, Belo Horizonte, 1ª edição, Editora O Lutador.

[19] Weng, C.C. and Yen, S.I. (2002). Comparisons of Concrete–encased Composite Column Strength Provisions of ACI Code and AISC Specification, v. 24, p. 59–72.

[20] Buildings code requirements for Structural Concrete (ACI 318–99) (1999). Detroit (MI): American Institute (ACI).

[21] Fong, M. (2012). Second–order analysis of imperfect light–weight and composite structures. Doctoral thesis, Department of civil and structural engineering, The Hong Kong Polytechnic University, Hong Kong, China.

[22] Sfakianakis, M.G. (2002). Biaxial bending with axial force of reinforced, composite and repaired concrete sections of arbitrary shape by fiber model and computer graphics. Advances in engineering software, v. 33, p. 227–242.